Journal of Catalysis **208,** 370–380 (2002)
doi:10.1006/jcat.2002.3580

Synergistic Catalysis of Carbon Monoxide Oxidation over Copper Oxide Supported on Samaria-Doped Ceria

Jenshi B. Wang,* De-Hao Tsai,† and Ta-Jen Huang†,[1]

*Department of Chemical Engineering, I-Shou University, Kaohsiung, Taiwan 840, Republic of China; and †Department of Chemical Engineering, National Tsing Hua University, Hsinchu, Taiwan 300, Republic of China

Received October 24, 2001; revised February 6, 2002; accepted February 19, 2002

Copper oxide supported on samaria-doped ceria (SDC) is chosen as a model catalyst for carbon monoxide oxidation to illustrate interfacial metal oxide–support interaction and synergism. The oxidation catalysis by CuO/SDC was studied to further elucidate the effect of oxygen vacancies on activity enhancement and light-off behavior. It was found that an approximate proportionality exists between the reducibility and the activity of catalysts. It is concluded that reducibility and susceptibility of change of oxidation states of copper oxides is key to catalytic activities, and the nonstoichiometric metastable copper oxide species formed during reduction are very active because of their superior capability to transport surface lattice oxygen. A preliminary mechanism involving surface lattice oxygen of CuO and oxygen vacancy participation is proposed to fully explicate the synergistic process leading to light-off. The cause of light-off is attributed to the formation of *co-shared* oxygen ions coupled with the creation of high-turnover-frequency active sites which are composed of metastable copper oxide species and oxygen vacancies of two types, $V_{o,CuO}$ and $V_{o,SDC}$. Over these CuO/SDC catalysts, the active sites exhibit the Langmuir–Hinshelwood-type mechanism characteristic of precious metals although the redox-cycle mechanism is still operative.

Key Words: **copper oxide; samaria-doped ceria; CO oxidation; synergism; surface lattice oxygen.**

1. INTRODUCTION

In exhaust emission control, to meet increasingly stringent environmental regulations in an economical way the complete oxidation of carbon monoxide is of prime importance. Precious metals have long been used as the most efficient oxidation catalysts with high activity and stability to control exhaust gas emissions. Due to the cost and limited availability of precious metals, considerable attention has been paid to transition metals and their oxides in these uses. Among base metals, copper has been explored as a possible substitute for precious metals because of its high activity toward CO oxidation (1, 2).

In addition, since the concepts of strong metal–support interaction (3, 4) and catalysis at the metal–support interface (5, 6) were introduced, supports have been studied to explore the advantages of the interaction in order to seek insight into developing new catalysts. Fluorite-type oxygen-ion-conducting oxides such as ceria, yttria-stabilized zirconia (YSZ), gadolinia-doped ceria, and samaria-doped ceria (SDC), when used as supports or catalysts, significantly enhance the catalytic activity of Pt (6), Rh (7), and CuO (8, 9) for CO oxidation and NO reduction. The improvements in catalytic activity by these oxides have been attributed to the oxygen storage/transport characteristics of the support (6, 7) and to the generation of very active centers existing at the interface between metal and support (8–11). Many studies have shown that the oxygen vacancies of metal oxides such as V_2O_5 (12) and CuO (13) play an important role in enhancing the catalytic activities of CO oxidation. A recent article by Dow and Huang (8) reported the effect of oxygen vacancies in YSZ on the activity enhancement and stability properties of copper catalysts for carbon monoxide oxidation.

Ceria has long been used as an effective component in automotive exhaust control using three-way catalysts because of its ability to store oxygen and improve dispersion of noble metals (14, 15). Doped ceria has been the subject of great interest because the addition of dopants greatly increases concentrations of oxygen vacancies (16), improves thermal stability of ceria (17), or enhances catalytic activity for CO oxidation and NO reduction (7). Rare earth oxides with trivalent cations are the best possible dopants for modifying structural and chemical properties of ceria because rare earth elements can easily replace cerium on its regular site (18). Copper oxide supported on doped ceria appears to provide an enhanced and unique catalytic property, that is, metal oxide–support synergism, to CO oxidation.

Countless works have been devoted to the study of carbon monoxide oxidation over copper catalysts because of its significance in understanding a number of major industrial applications, in addition to exhaust emission control. It has been generally agreed that CO oxidation over copper

[1] To whom correspondence should be addressed. Fax: 886-3-571-5408. E-mail: tjhuang@che.nthu.edu.tw.

0021-9517/02 $35.00

oxide catalyst involves surface oxygen/oxygen vacancy participation (19–21). However, to date, there is a dearth of information on the interaction of fluorite-type oxygen-ion-conducting oxide supports with base metal catalytic agents for CO oxidation. As a result, even though significant enhancement in CO oxidation activity over copper supported on doped oxide has been recognized, its mechanism remains poorly understood. Liu and co-workers (22) arrived at the conclusion that copper in Cu-promoted ceria catalysts for CO oxidation existed in the form of clusters which were stabilized by "strong interaction" with the cerium oxide matrix. In work by Dow and Huang (8), the catalytic activity enhancement of CO oxidation was attributed to the surface oxygen vacancies of YSZ and to the synergism brought about by the interfacial metal oxide–support interaction (IMOSI). A very recent study by Wang *et al.* (9) ascribed the synergistic effect enhancing CO oxidation activity to the formation of interfacial active centers between copper oxide clusters and SDC support but gave no detail about the involvement of surface lattice oxygen of copper oxide and did not elaborate on mechanistic schemes at all.

The purpose of this work is to focus on CO oxidation over copper oxide catalysts supported on fluorite-type oxygen-ion-conducting oxides to further elucidate the effect of oxygen vacancies on activity enhancement and light-off behavior. A preliminary mechanism involving surface lattice oxygen of CuO and oxygen vacancy participation is proposed to fully explicate the synergistic process leading to light-off. CuO/SDC was employed as a model catalyst since the samaria–ceria system reportedly displayed superior ionic conductivity (23), and CuO/SDC was demonstrated to exhibit excellent activity for CO oxidation (9). Activity evaluations coupled with CO-temperature-programmed reduction were carried out to study the oxidation properties of the model catalyst. We hope this preliminary study will aid the development of a better understanding of the synergism between the copper oxide species and the oxide support brought about by IMOSI.

2. EXPERIMENTAL

2.1. Catalyst Preparation and Characterization

SDC was prepared from reagent-grade (99% purity, Strem Chemical Co.) metal nitrates $Sm(NO_3)_3 \cdot 6H_2O$, $Ce(NO_3)_3 \cdot 6H_2O$ by a coprecipitation method. Appropriate amounts of samarium nitrate and cerium nitrate were dissolved in deionized water to make 0.08 M solutions. Hydrolysis of the metal salts to hydroxides was obtained by adding NH_4OH solution and in the meantime stirring to keep the pH of the solution greater than 9. A distinct deep purple color of precipitate/gel was formed when NH_4OH was added into the nitrate solution. Vacuum filtration was employed to isolate the gel, which was then washed twice by water and ethanol. After washing, the gel was dried under vacuum at 110°C for 4 h, calcined in air at 300°C for 2 h and at 700°C for 4 h, and then immediately quenched in water.

The copper catalysts were prepared by impregnating SDC support with an appropriate amount of aqueous solution of copper nitrate trihydrate (SHOWA, Japan). After excess water was evaporated at 80°C, the catalysts were dried under vacuum at 80°C for 12 h, and then calcined in air at 260°C for 1.5 h and at 500°C for 3.5 h. The calcination of the supports and catalysts was conducted by passing air at the rate of 1 L/min and by raising the temperature from room temperature at a rate of 10°C/min . Powdered samples of Cu (99% purity, Aldrich), Cu_2O (99.5%, SHOWA), and CuO (98.5%, SHOWA) were ground to be used in temperature-programmed reduction studies.

2.2. Definition of Catalyst Symbols

1. The number in front of Cu is the copper loading in weight percent, which is calculated with respect to the weight of the SDC support.
2. The number before SDC is the samaria content in mole percent, which is evaluated based on moles (samarium plus cerium) of SDC.

2.3. Activity Measurement

The time-on-stream activity tests of the catalysts were conducted for 360 min under atmospheric pressure in a continuous-flow reactor charged with 0.3 g of catalyst. The reactor was an 8-mm-ID Pyrex U-tube imbedded in a silica–oil circulating tank (Mandarin Scientific Co.). Two K-type thermocouples were employed. One was placed in the silica–oil bath to monitor and control the bath temperature, while the other was inserted into the catalyst bed to measure the reaction temperature in the bed.

Two reaction atmospheres were adopted for the test, a gas mixture composed of 1.80% CO plus 2.95% O_2 in argon for oxygen rich, and 1.85% CO, 0.56% O_2, and the balance argon for oxygen lean environments, both at a total flow rate of 300 ml/min. The flowing of the reactants, CO (99.9% purity, Air Products), O_2 (99.995%), and Ar (99.9995%), was regulated by mass flow controllers (Hastings, Model HFC-202). The reactor outflow was analyzed online by a CO-NDIR (Beckman 880), a gas chromatograph (Shimadzu GC-8A) equipped with a thermal conductivity detector, and an oxygen analyzer (Beckman 755A). Both the signals of CO-NDIR and the temperatures of the catalyst bed were transmitted to a Y-t recorder (Yokogawa, LR-4110).

2.4. CO-Temperature-Programmed Reduction (CO-TPR)

The CO-TPR was carried out by using CO of different percentages in argon as a reducing gas to obtain reduction data more related to the catalytic oxidation of CO. The TPR reactor was made up of an 8-mm-ID quartz U-tube with

catalyst samples of varying weights mounted on loosely packed quartz wool. The flow rate of the reducing gas was kept at 44 ml/min by a mass flow controller. The temperature of the reactor was increased from room temperature to 550°C at a rate of 10°C/min by a temperature-programmable controller (Eurotherm, 815P). The rate of CO consumption was analyzed by a CO-NDIR and recorded by an online personal computer. The peak areas of TPR were separated and integrated using software developed by SISC, Taiwan.

3. RESULTS

3.1. CO-TPR of Copper(I) and Copper(II) Oxides

A γ-reduction peak appeared in the CO-TPR patterns of CuO as shown in Fig. 1. The appearance of the reduction peak indicated that metallic copper had been formed directly from carbon monoxide reduction of copper(II) oxide (24, 25). The peak temperature and area under the peak increased with the increase in copper(II) oxide loadings, which seemed to have negligible effect on the temperature at which reduction began.

Figure 2 depicts the TPR profiles of copper(II) oxide over three reduction atmospheres. With the increase in CO concentration, the reduction peak became sharper and moved toward lower temperatures, while the low-temperature-reduction area (the portion to the left of the dashed line in the figure) increased. This suggests that the reducibility of copper(II) oxide in the early phase of reduction is approximately proportional to the concentration of the reducing gas.

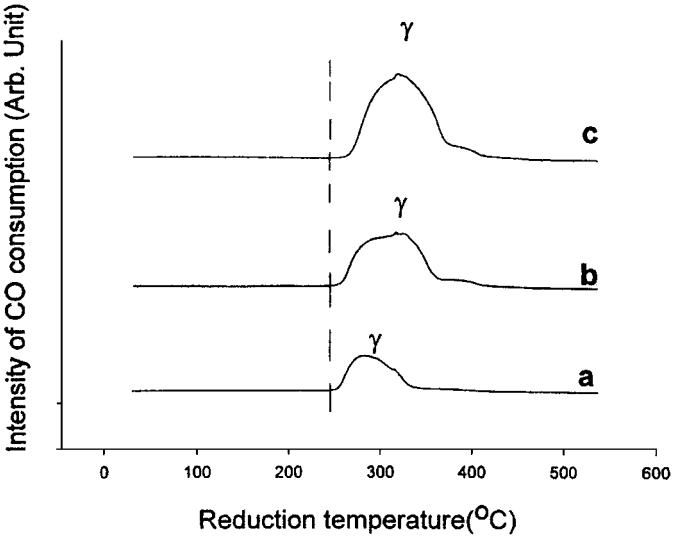

FIG. 1. CO-TPR patterns of CuO. Operating conditions: 10°C/min, 1.70% CO in Ar with total flow rate of 44 ml/min. Sample weight: (a) 4.6, (b) 10.1, and (c) 15 mg.

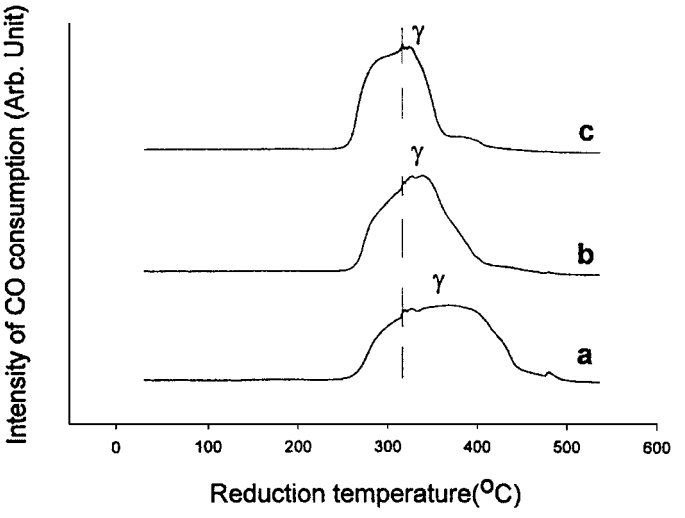

FIG. 2. CO-TPR patterns of CuO. Operating conditions: 10°C/min; total flow rate, 44 ml/min; sample weight, 10.1 mg. Reduction atmosphere: (a) 0.67% CO in Ar, (b) 1.13% CO in Ar, and (c) 1.70% CO in Ar.

In order to have more understanding of the activity of the oxidation states of copper, the CO-TPR of copper(I) oxide was carried out as shown in Fig. 3. Comparison of profile a with profiles b and c, and relating profile b to profile e, shows that the effects of copper(I) oxide loading and CO concentration were analogous to those of copper(II) oxide, as shown in Figs. 1 and 2, respectively. However, more than one reduction peak was observed in the TPR patterns of Cu_2O, which implied that other reduction states existed

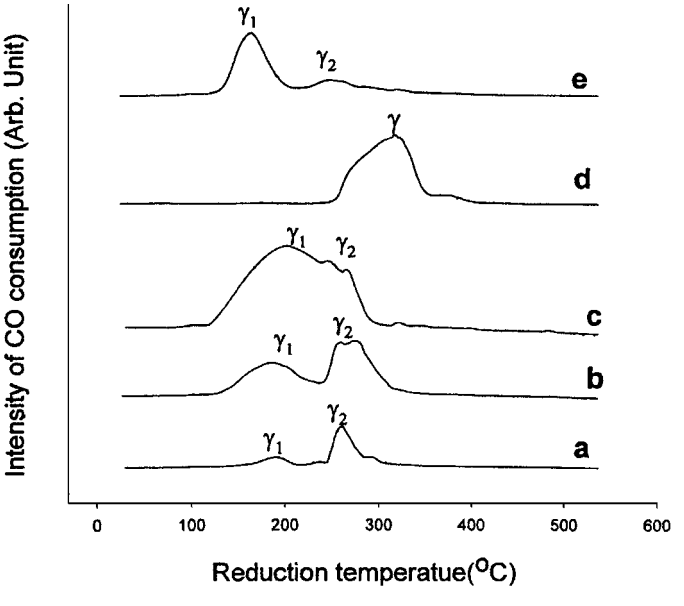

FIG. 3. CO-TPR patterns. Operating conditions: 10°C/min; total flow rate, 44 ml/min. (a) Cu_2O, 4.6 mg, 1.13% CO in Ar; (b) Cu_2O, 14 mg, 1.13% CO in Ar; (c) Cu_2O, 27 mg, 1.13% CO in Ar; (d) CuO, 7.5 mg, 1.70% CO in Ar; (e) Cu_2O, 14 mg, 1.70% CO in Ar.

during the course of reduction (24). Since cuprous oxide when exposed to air is susceptible to being oxidized, it is presumed that the second reduction peak, γ_2, was due to the air exposure of the oxide during sample weighing and handling.

A comparison of profiles Fig. 1a and Fig. 3a shows that the γ_1 reduction peak of Cu_2O occurred at a much lower temperature than that of CuO. This indicates that Cu_2O is more easily reduced than CuO. However, CuO displayed higher peak area, which is natural because, on the basis of the same weight, CuO possesses more lattice oxygen than Cu_2O does. If we consider Figs. 3d and 3e, which have the same number of moles, or equivalently the same number of lattice oxygens, it appears that these two oxides had no appreciable difference in total peak areas, whereas the peak temperatures of Cu_2O were lower than that of CuO. Accordingly, it becomes apparent that Cu_2O starts to be reduced at much lower temperatures than CuO, and thus Cu_2O is considered to exhibit a higher reducibility than CuO.

3.2. *CO-TPR and Activity Tests of CuO/SDC Catalysts*

For the CuO/SDC catalysts studied in this work, especially the high-copper-content xCu/10SDC samples, the presence of bulk CuO phase can be verified by the XRD spectra of 5Cu/10SDC/γ-Al_2O_3 and 7Cu/10SDC/γ-Al_2O_3 samples reported earlier (9, 26), in which the diffraction peaks characteristic of copper oxide could be easily discriminated. As displayed in Fig. 4, three peaks, α, β, and γ, could be distinguished in the CO-TPR profiles of xCu/10SDC catalysts. It is clearly observable that in pure SDC support no reduction peak appeared below 500°C, so that the formation of α, β, and γ peaks was obviously due to the reduction of supported CuO. The area of $\beta + \gamma$ peaks increased with increasing copper loading, which seems to have little effect on the inception temperature of α-peak reduction. This is expected since the formation of the α peak at low temperature was attributed to the CO consumption of interfacial oxygen ions of the copper oxide species interacting with the surface oxygen vacancies of ceria in SDC, i.e., the effect of IMOSI (9). The amount of these copper oxide species is measured by the α-peak area. Thus, for quantitative analysis, all of the reduction peaks were integrated to evaluate the absolute and fractional α-peak areas, which are listed in Table 1. The absolute α-peak area increased with the increase in CuO loading. The increase in α-peak area is clearly a result of the increasing copper oxide species interacting with the surface oxygen vacancies of ceria in SDC.

TABLE 1

The Integrated Values of CO-TPR Peaks of CuO/SDC Catalysts[a]

Catalyst	Absolute amount of α peak (mol CO)	Fraction of α peak[b] (%)
2.5Cu/10SDC	5.95E-06	15.11
5Cu/10SDC	8.66E-06	11.00
7.5Cu/10SDC	1.10E-05	9.27

[a] Operating conditions of CO-TPR: 10°C/min; 1.13% CO in Ar with total flow rate of 44 ml/min; sample weight, 0.1 g.

[b] Fraction of α peak = (α peak area)/(total peak area of CuO) × 100%.

Figure 5 shows the activities of CO oxidation catalyzed by CuO/SDC with different copper loadings under oxygen-rich conditions. It is interesting to observe that the CO oxidation activity was enhanced with the increase in copper

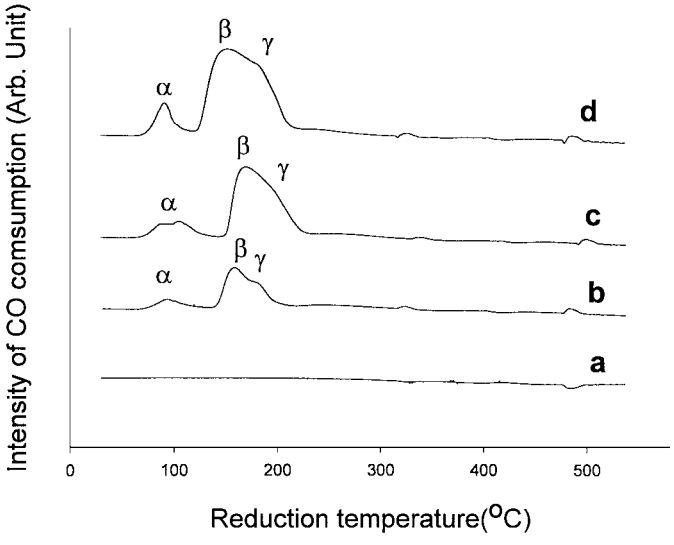

FIG. 4. CO-TPR patterns of CuO/SDC. Operating conditions: 10°C/min; 1.13% CO in Ar with total flow rate of 44 ml/min; sample weight, 0.1 g. Support and catalysts: (a) SDC support, (b) 2.5Cu/10SDC, (c) 5Cu/10SDC, and (d) 7.5Cu/10SDC.

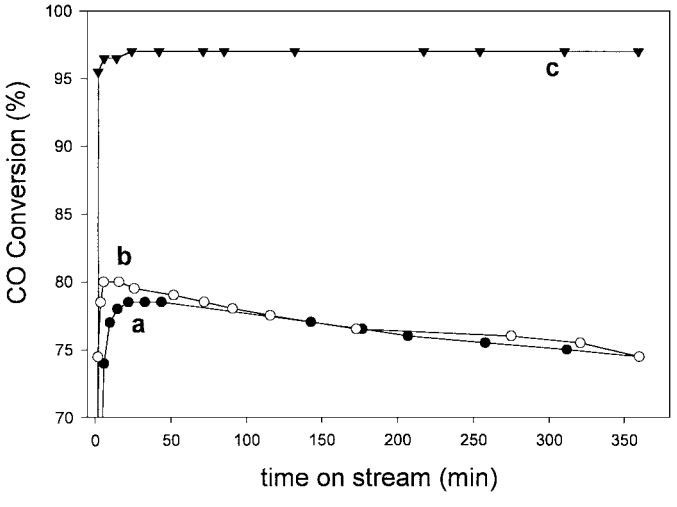

FIG. 5. Activity behavior of CuO/SDC under oxygen-rich conditions. Sample weight, 0.3 g; reaction temperature, 175°C. Catalysts: (a) 2.5Cu/10SDC, ●; (b) 5Cu/10SDC, ○; and (c) 7.5Cu/10SDC, ▼.

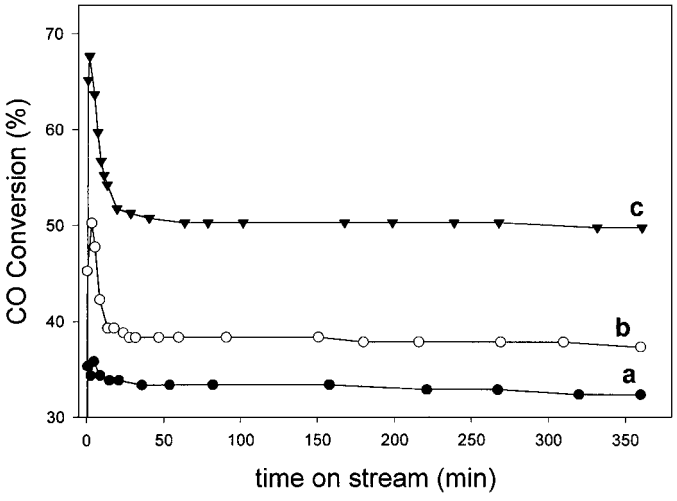

FIG. 6. Activity behavior of CuO/SDC under oxygen-lean condition. Sample weight, 0.3 g; reaction temperature, 175°C. Catalysts: (a) 2.5Cu/10SDC, ●; (b) 5Cu/10SDC, ○; and (c) 7.5Cu/10SDC, ▼.

loading, and a sharp rise in activity, right after the reaction was started, occurred for every catalyst exhibiting the light-off behavior characteristic of precious metal catalysts. Catalyzed by CuO/SDC in an oxygen-lean environment, the conversion of CO increased drastically at the outset of the reaction and then declined to a steady one, as depicted in Fig. 6. It is also seen that the catalytic activity of CO conversion increased with an increase in copper loadings.

From Figs. 5 and 6, it is obvious that the order of activity among the catalysts was independent of the prevailing oxygen concentration in the reaction. In addition, the orders of activity coincide well with the sequence of α-peak areas shown in the TPR profiles of Fig. 4. This again asserts that the IMOSI resulting from CuO/SDC interaction is the driving force leading to activity enhancement.

4. DISCUSSION

Synergistic effects between metal/metal oxide and support leading to catalytic activity enhancement of CO oxidation have been studied extensively. The activity enhancement was ascribed to the formation of active sites, at which the turnover frequency is very high, between metal/metal oxide particles and the support (6, 8, 27, 28). The interfacial active sites and CO activity enhancement which result from synergism and interaction between copper oxide and SDC support have recently been investigated, but with no elaboration on catalytic mechanisms (9). In this work, using CuO/SDC as a model system, we elucidate a catalytic mechanism involving surface lattice oxygen of CuO and participation of oxygen vacancy leading to activity enhancement and light-off behavior. Further discussions on the reduction of copper oxide species, which is of prime importance at the inception stage of CO catalytic oxidation, and on the reduction behavior of CuO/SDC catalysts are also provided.

4.1. Light-Off Behavior of CuO/SDC Catalysts

As shown in Figs. 5 and 6 regarding the activity of CuO/SDC catalysts, a correlation exists between the activity and the reducibility of catalysts, and a light-off behavior occurs in the presence of rich oxygen. Figure 7 reveals that the CuO/SDC-catalyzed CO oxidation behavior over time-on-stream is quite different from that catalyzed by CuO. Over CuO/SDC, in contrast to that catalyzed by CuO, no induction period existed and the CO concentration

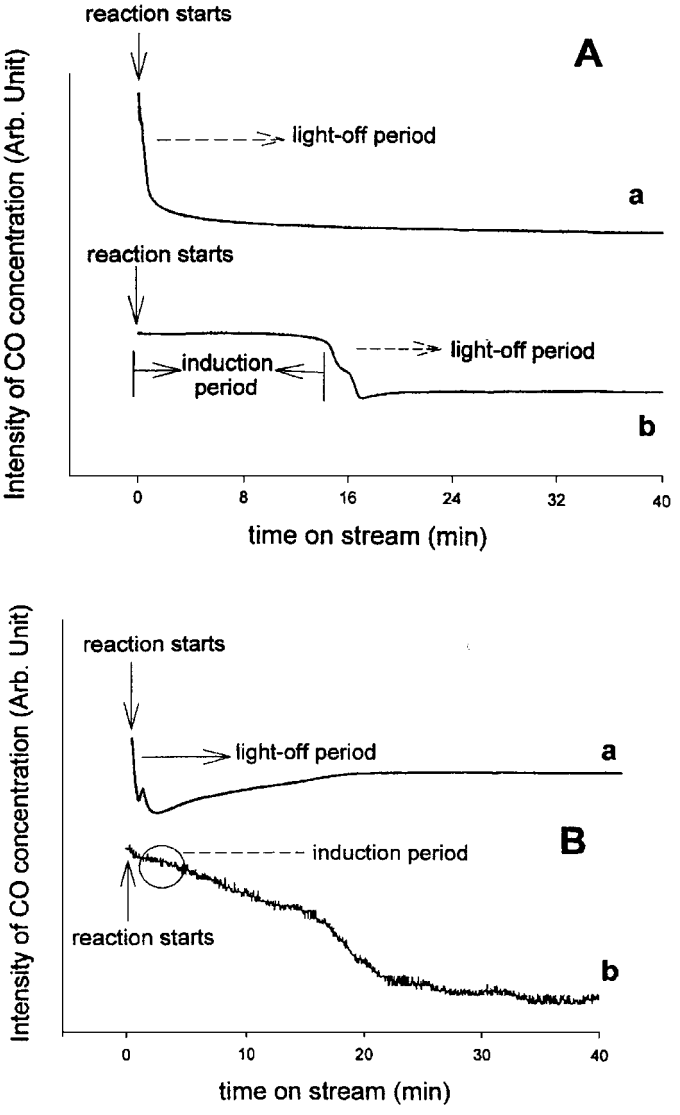

FIG. 7. Variations of catalytic behavior exhibited by (a) CuO supported on an oxygen-ion-conducting material, SDC; (b) pure CuO. (A) Oxygen rich; (B) Oxygen lean. All samples have the same loading of copper(II) oxide.

dropped sharply soon after the reaction was started. These striking differences in activity behavior can be attributed to the effect of IMOSI induced by the oxygen-ion-conducting support, SDC (3). In general, CO oxidation over base–metal oxide catalysts follows the Mars–van Krevelen redox mechanism (1, 29–32). Jernigan and Somorjai (30) indicated that the redox mechanism for CO oxidation over CuO catalyst cycles between CuO and Cu_2O where the rate-limiting step is the reduction of copper(II) oxide by CO.

Oxygen-ion-conducting material such as ceria was used successfully to improve the catalytic activity of precious metal catalysts, inhibited by strong adsorption of CO at low temperatures, by providing interfacial lattice oxygen. An interfacial oxygen vacancy would thus be created after the interfacial lattice oxygen of ceria had been removed by the interfacial metal-adsorbed CO. Over CuO/YSZ, Dow and co-workers (8, 33) proposed a mechanism of CO oxidation that involves the nested oxygen ion reacting with CO to produce CO_2, thus forming an interfacial active center. In a recent investigation the oxygen vacancies of SDC were reported to play a vital role in CO oxidation activity enhancement by CuO/SDC due to the synergistic effect of copper oxide and the oxygen vacancies of SDC by means of formation of interfacial active centers (9). Details of this mechanism involving redox cycle and active center participation leading to activity enhancement and light-off behavior are proposed as follows and are shown in Fig. 8.

Step a: The CuO/SDC catalyst at the outset of reaction.

Steps b–c: The nested oxygen ion of CuO neighboring with the oxygen vacancy of SDC ($V_{o,SDC}$) is attacked by CO, so that CuO is reduced to a transient Cu^0. An oxygen vacancy of CuO ($V_{o,CuO}$) is thus formed at this step:

$$\begin{aligned} &Cu^{2+}\ldots O^{2-}\ldots Cu^{2+}\ldots O^{2-}\ldots V_{o,SDC} + CO \\ &\quad\rightarrow Cu^{2+}\ldots O^{2-}\ldots Cu^{0} + CO_2 + V_{o,SDC} + V_{o,CuO}. \end{aligned} \quad [1]$$

Steps a–c have been proposed and confirmed by Dow and Huang (8) and Wang *et al.* (9) for supports of YSZ and SDC, respectively. Jernigan and Somorjai (30) have shown similarly that CO_2 production must result from the surface reduction of copper(II) oxide by CO. The CO-TPR result in Fig. 4 shows that two types of reduction behavior exist and, according to Dow *et al.* (33) and Wang *et al.* (9), the α-type reduction that easily occurs at low temperatures is the major behavior of reaction [1]. This agrees with studies (25, 34–36) showing that the reduction of CuO may proceed directly to Cu at temperatures below 200°C without undergoing two steps, i.e., $Cu^{2+} \rightarrow Cu^{+} \rightarrow Cu^{0}$. As a result, reaction [1] proposed in the mechanism is reasonably established.

Steps c–d: The transient Cu^0 will be affected by the neighboring oxygen ions, and formation of $Cu^{+}\ldots O^{2-}\ldots Cu^{+}$, due to electron transfer in the metastable cluster of copper oxide, follows afterward:

$$Cu^{2+}\ldots O^{2-}\ldots Cu^{0} \rightarrow Cu^{+}\ldots O^{2-}\ldots Cu^{+}. \quad [2]$$

As the reduction takes place, the CuO clusters become metastable because the loss of lattice oxygen results in unbalanced total valences in the clusters. Severino *et al.* (25) indicated that the dominant species present in CO-pretreated catalysts was Cu^0, which was then transformed to a mixture of Cu^0 and Cu^+ species when exposed to $CO + O_2$ under reaction conditions. Other authors (37–39) have also proposed the coexistence of Cu^0 and Cu^+ over supported CuO catalyst. Thus, an extended agreement seems to exist in the literature that both Cu^0 and Cu^+ are essential for CO oxidation on copper-based catalysts (40–42). Once the copper is reduced to Cu^0 in the prereduction step, the reduced surface is partially oxidized during the course of reaction, and formation of Cu^+ to some extent will occur. Liu *et al.* (22) further identified by XPS the formation of Cu^+ species in their study of the interaction of fluorite oxides with copper catalysts for CO oxidation. Thus, the proceeding of reaction [2] can be readily concluded.

Since having copper partly in the +1 state is essential for the catalytic activity, it is conceivable that the activity will be enhanced appreciably when Cu^+ is formed in the CuO cluster. Sadykov and Tikhov (43) pointed out the existence of an oxygen defect phase which occurs as a metastable state and influences catalytic activity. Nagase *et al.* (44) have proposed that the occurrence of a metastable cluster, including an oxygen vacancy, is the active site in the reaction. Pierron *et al.* (36) reported that CO reduction of cupric oxide resulted in the generation of reduced copper phases and the formation of lattice heterogeneities. And Dekker and coworkers (45) have shown that over copper-based catalysts possible redox couples are Cu^+–Cu^{2+}, Cu^0–Cu^{2+}, and Cu^+–Cu^0. In sum, owing to electron transfer the nonstoichiometric clusters, composed of ion pairs such as Cu^0–Cu^{2+}, Cu^+–Cu^{2+}, Cu^+–Cu^+, and Cu^+–Cu^0, are very active because of their superior redox capability. Therefore, reaction [2] represents the electron transfer in the metastable cluster.

Step d: CO prefers to be adsorbed to the metastable copper cluster, while O_2 is drawn to the oxygen vacancies that would be a good adsorption site for oxygen.

Step e: The dissociative adsorption of O_2 occurs on the oxygen vacancies of SDC and CuO, the latter having just been formed by CuO reduction at steps b–c. CO adsorbs on the metastable copper cluster:

$$2V_{o,CuO} + O_2 \rightarrow 2V_{o,CuO}\ldots O \quad [3]$$

$$2V_{o,SDC} + O_2 \rightarrow 2V_{o,SDC}\ldots O \quad [4]$$

$$Cu^{+}\ldots O^{2-}\ldots Cu^{+} + CO \rightarrow Cu^{+}\ldots O^{2-}\ldots Cu^{+}\ldots CO. \quad [5]$$

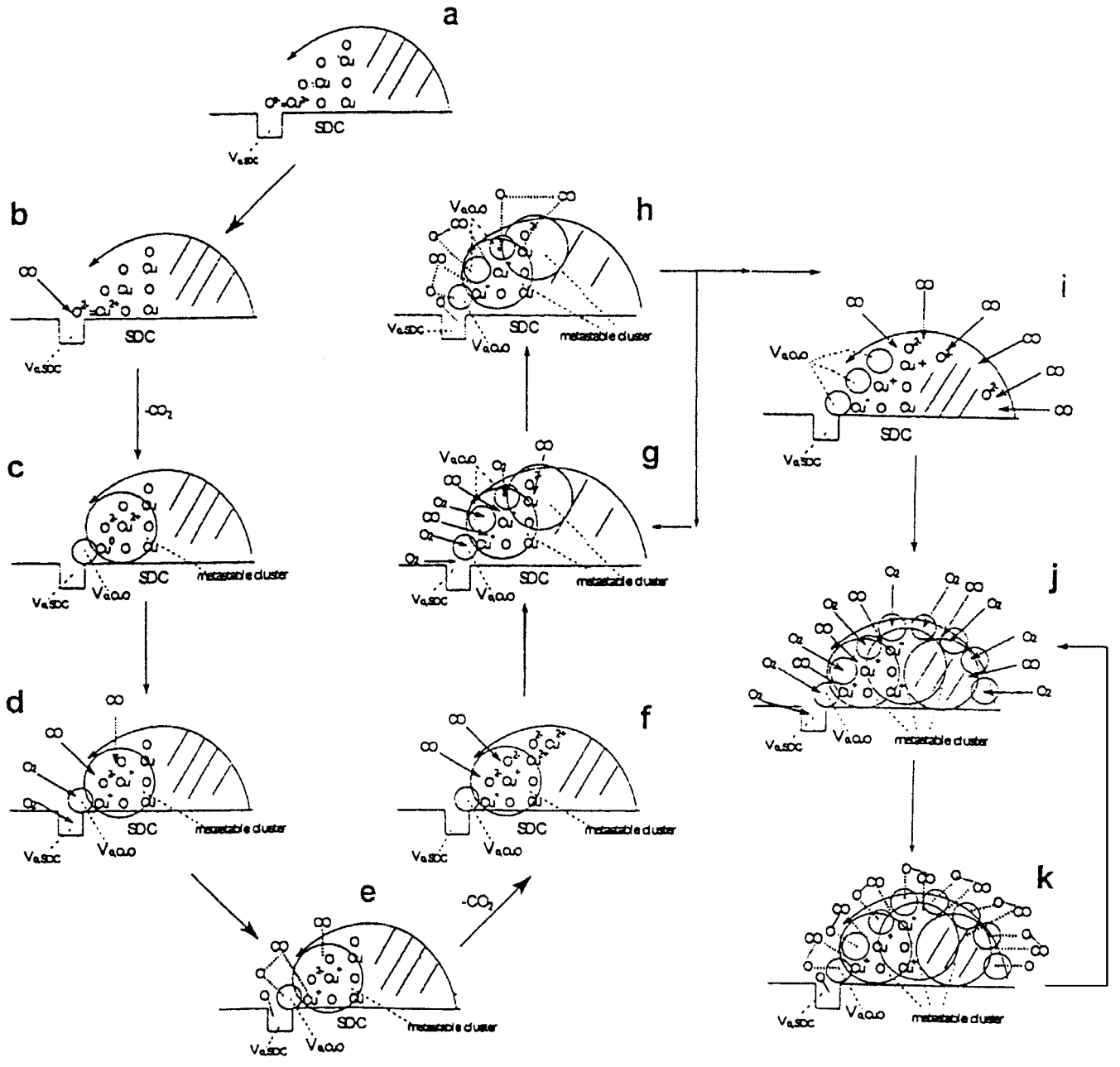

FIG. 8. The mechanism of CO oxidation over copper oxide supported on an oxygen-ion-conducting material, SDC. Steps a–k: described in text.

Zhang *et al.* (46) pointed out that the oxygen vacancies of oxygen-ion-conducting solids make suitable sites available for oxygen adsorption. These authors further concluded that the common features of oxygen chemisorption on the oxygen-ion-conducting materials might be (i) the high capacity for oxygen adsorption, and (ii) the tendency to form atomic-type oxygen species on the surface. Dow and Huang (8) indicated that oxygen vacancies acted as good defect sites for the adsorption of atomic-type oxygen species. Moreover, Mergler *et al.* (47) suggested that for CO oxidation, oxygen vacancies on the metal oxide play an important role as dissociation centers for O_2. O_2 dissociation only occurs when electrons are donated from the surface to the O_2 molecule, leading to a metal cation and oxygen anion pair. Because of these studies, coupled with other investigations (6, 35, 40), reactions [3] and [4] are readily verified with the existence of oxygen vacancies. Considering the chemisorption character of CO, owing to the lone pair of electrons on carbon, CO prefers to adsorb on the nonstoichiometric copper cluster (48). Accordingly, the copper cluster, which can supply electron holes, will give a higher activity for the

donor-type reaction of CO, such as the one shown in reaction [5].

Steps e–f: The "co-shared" oxygen ions are formed between the oxygen vacancies and the adsorbed CO and then reacted with the adsorbed CO to form CO_2 which then desorbs:

$$\mathrm{Cu^+ \ldots O^{2-} \ldots Cu^+ \ldots CO} + V_{\mathrm{o,CuO}} \ldots \mathrm{O} \rightarrow \mathrm{Cu^+ \ldots O^{2-} \ldots Cu^+ \ldots CO \ldots O} \ldots V_{\mathrm{o,CuO}} \quad [6]$$

$$\mathrm{Cu^+ \ldots O^{2-} \ldots Cu^+ \ldots CO} + V_{\mathrm{o,SDC}} \ldots \mathrm{O} \rightarrow \mathrm{Cu^+ \ldots O^{2-} \ldots Cu^+ \ldots CO \ldots O} \ldots V_{\mathrm{o,SDC}} \quad [7]$$

$$\mathrm{Cu^+ \ldots O^{2-} \ldots Cu^+ \ldots CO \ldots O} \ldots V_{\mathrm{o,CuO}} \rightarrow \mathrm{Cu^+ \ldots O^{2-} \ldots Cu^+} + \mathrm{CO_2} + V_{\mathrm{o,CuO}} \quad [8]$$

$$\mathrm{Cu^+ \ldots O^{2-} \ldots Cu^+ \ldots CO \ldots O} \ldots V_{\mathrm{o,SDC}} \rightarrow \mathrm{Cu^+ \ldots O^{2-} \ldots Cu^+} + \mathrm{CO_2} + V_{\mathrm{o,SDC}}. \quad [9]$$

As a description comparable to the Langmuir–Hinshelwood (L–H)-type mechanism of precious metal catalysts, the above behavior is stated as being that CO adsorbs on the active site of the CuO/SDC surface and reacts with the neighboring $O_{(ad)}$ at the interface between CuO and SDC. Many studies have verified that these interfacial reactions have an appreciable contribution for CO oxidation over Pt and Pd catalysts (6, 27, 28) and over CuO/YSZ catalysts (8), leading to a higher initial activity.

Steps f–g: Additional molecules of CuO neighboring with oxygen vacancy of CuO ($V_{\mathrm{o,CuO}}$) are reduced by CO, forming more metastable clusters and oxygen vacancies.

Steps g–h: More reactant molecules participate and react.

The reaction sequence of [6]–[9] is considered to be due to the formation of coshared oxygen ions, igniting neighboring sites to create additional oxygen vacancies consecutively. The reaction spreads out from the interface between CuO and SDC to the surface of the $(\beta+\gamma)$-type CuO cluster, defined as those copper species with $(\beta+\gamma)$-type reduction in the foregoing CO-TPR results, bringing about further formation of active sites.

Steps a–h can be viewed as the induction mechanism for the CuO/SDC catalyst, for which, after the reduction is triggered by surface defects, the induction proceeds very rapidly, thereby drastically reducing its induction period, as depicted in Figs. 5, 6, and 7. The repetition between steps g and h persists until the reaction condition reaches that suitable for the occurrence of light-off. This repetition is regarded as the incubation of light-off, the mechanism of which is exemplified by steps i–k.

Steps i–j: The number of reduced CuO and oxygen vacancies of CuO multiplies, creating active sites in large quantities:

$$x\mathrm{Cu^{2+} \ldots O^{2-} \ldots Cu^{2+} \ldots O^{2-}} + x\mathrm{CO} \rightarrow x\mathrm{Cu^+ \ldots O^{2-} \ldots Cu^+} + x\mathrm{CO_2} + xV_{\mathrm{o,CuO}}. \quad [10]$$

In the CO-TPR of CuO/SDC, the $(\beta+\gamma)$-type reduction of the CuO cluster is looked upon as the major characteristic of the light-off behavior represented by reaction [10]. As elaborated in reaction [2] above, reaction [10] also involves electron transfers in CuO clusters. Note that reaction [10] is similar to reactions [1]–[2] without the participation of the oxygen vacancies of SDC. Thus, it may occur over unsupported copper catalysts. It is apparent that the key points for the occurrence of light-off in the CO oxidation over the CuO/SDC catalyst is the formation of oxygen vacancies of CuO and then fast turnover of the adsorbed reactants on the active sites associated with these oxygen vacancies.

Step k: Substantial "co-shared" oxygen ions are being formed and then converted to CO_2, liberating far more active sites to sustain the reaction.

The repetition between steps j and k sustains the reaction at high conversions after light-off takes place. As shown in Fig. 5, the fact that the activities of CuO/SDC catalysts jumped drastically soon after the reaction was started and then was maintained at a roughly steady value provides clues for the assumption of repetition between j and k. Due to this repetition, the turnover frequency increases considerably so that the activities and conversions can be maintained at elevated levels.

Based on the above arguments, it is suggested here that for CO oxidation catalyzed by copper oxide supported on oxygen-ion-conducting materials, once ignited by the surface oxygen vacancies of the latter, the activity enhancement and light-off behavior can be attributed to the oxygen vacancies of CuO and the $(\beta+\gamma)$-type CuO clusters. The active sites which are composed of metastable copper clusters and two types of oxygen vacancies ($V_{\mathrm{o,CuO}}$, $V_{\mathrm{o,SDC}}$) exhibit the L–H-type mechanism of precious metals, although the redox-cycle mechanism is still operative in the reaction over the CuO/SDC catalysts since CuO/SDC still displays CO oxidation activity in the absence of O_2, as evidenced by the results of Fig. 4. Over CuO/YSZ, Dow and Huang (8) also observed that CO oxidation by surface lattice oxygen could not be neglected, especially for high copper loadings.

4.2. Reduction of Copper Oxides

For CO oxidation over copper oxide catalysts, it is generally agreed that the reaction obeys a redox cycle mechanism (32),

$$\mathrm{CO} + \mathrm{O_{SL}} \rightarrow \mathrm{CO_2} + \square_{\mathrm{s}}, \quad [11]$$

$$\mathrm{O_2} + \square_{\mathrm{s}} \rightarrow 2\mathrm{O_{SL}}, \quad [12]$$

where O_{SL} is a surface lattice oxygen and $\square_s$ is a surface oxygen vacancy on the metal oxide surface. Usually, reoxidation of the catalytic surface, reaction [12], is rather fast and thus oxygen withdrawal from the metal oxide,

reaction [11], appears to be the rate-determining step (29–31). The reaction rate will be enhanced when more surface lattice oxygen is withdrawn from the metal oxide.

From the viewpoint of catalytic oxidation reaction, if the reaction is of a redox mechanism, weaker bond strength of oxygen ions usually leads to more significant activity enhancement, which has been verified for many reactions (32, 49, 50). These findings suggest that the weakly bound oxygen ions could be removed more easily. For the same reason, if weakly bound oxygen ions exist on the surface of the metal oxide, the reduction of the metal oxide will readily take place at this position. From the CO-TPR shown in Fig. 3, the fact that the reduction of Cu_2O occurred in the low-temperature regime well before the incipience of CuO reduction implies that Cu_2O is more easily reduced and its surface lattice oxygen is more liable to come loose.

Nagase *et al.* (44) proposed that variations in copper valence during CO oxidation over CuO and Cu_2O cycled between II and 0 for CuO, while for Cu_2O the valence changed from I to II first and then cycled between II and I. This result coupled with the discussion above suggests that the rates of CO oxidation over different copper oxide species are different. On the basis of the same weight, CuO possesses more lattice oxygen, or equivalently more surface lattice oxygen, than Cu_2O. Under oxygen-rich conditions, there is no change in the oxidation state of CuO, but Cu_2O and Cu are oxidized partially to increase their surface lattice oxygen. On the other hand, under oxygen-lean conditions, CuO and Cu_2O are liable to be reduced to lower oxidation states, resulting in the loss of surface lattice oxygen. With this in mind, one can elucidate the activity scenario in terms of the role that variations of oxidation states of copper would play during CO oxidation. The valence variation of copper is accompanied by a change in the number of surface lattice oxygens. Thus, the oxidation activity of copper oxide species depends on their ability to transport surface lattice oxygen.

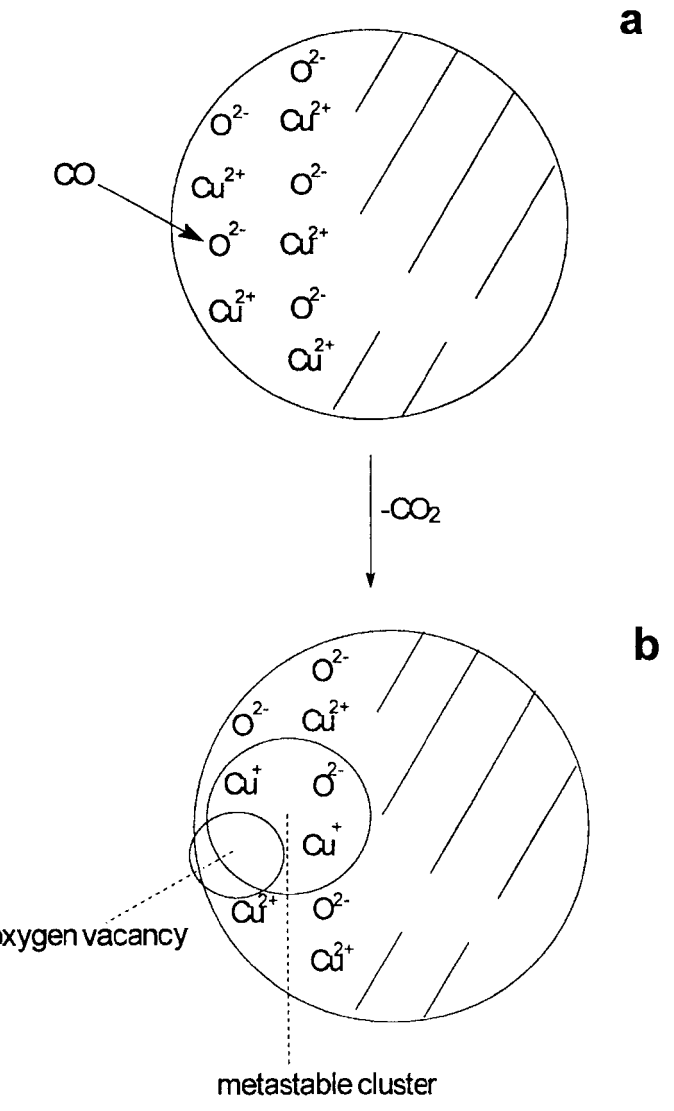

FIG. 9. Reduction scheme of CuO.

4.3. Reduction Behavior of CuO/SDC Catalysts

The reduction of a metal oxide by CO is, in a general sense, a heterogeneous catalytic reaction involving CO and oxygen ions of the metal oxide. Based on the concept of a heterogeneous catalytic reaction, if a very active site exists on the surface of the metal oxide, the reduction will take place easily and occur at lower temperatures. In other words, the reduction of the metal oxide needs some starting points, and the "trigger" of the reduction reaction may be a defect such as a surface oxygen vacancy or a weakly bound surface oxygen ion.

There is no trigger present in CuO at the outset of the reaction, for which the rate-determining step is to form a trigger such as oxygen vacancies on the CuO surface. It is presumed that the reduction of CuO is initiated at the surface of the copper cluster, as illustrated in Fig. 9. Similar arguments have been given in the literature. Boon and co-workers (13) have confirmed that surface oxygen vacancies of copper oxide are the active sites for the TPR of the supported copper oxides. Lo Jacono *et al.* (35) pointed out that a good adsorption site for the reduction of the alumina-supported copper oxide involved special configurations, such as coordinatively unsaturated surface Al^{3+} ions, close to edges or other defects. As triggers, i.e., oxygen vacancies, are formed, the valences of copper around the triggers are changing, so that the copper oxide cluster becomes unstable. The metastable cluster, made up of ion pairs such as Cu^0–Cu^{2+}, Cu^+–Cu^{2+}, and Cu^+–Cu^0 (45), is susceptible to being reduced or oxidized to other oxidation states. The metastable cluster of CuO is very active because of its superior ability to transport surface lattice oxygen, and the activity of catalysts will be significantly enhanced when nonstoichiometric copper oxides are formed.

For CuO/SDC catalysts, the occurrence of β and γ peaks has been ascribed to the reduction of highly dispersed copper oxide species and bulklike CuO, respectively, and is considered an intrinsic behavior of copper oxide (33). However, as shown in Fig. 4, these reduction-peak temperatures are much lower than those of unsupported CuO, such as those shown in Fig. 2. This behavior is associated with the formation of the α peak. Unlike inert supports, SDC provides active sites good for oxygen adsorption, so that the surface lattice oxygen of CuO neighboring the support is liable to be seized and carried away from the bulk CuO by the reducing gas (8, 51). In this regard, Wang and co-workers (9) have reported that the downward shift in reduction peak temperatures is because of improved dispersion of copper oxide through interaction with the oxygen vacancies of SDC. Differently from the cases of β and γ peaks, the α-peak temperatures are almost not affected by reduction atmospheres and copper loadings, as revealed by Fig. 4. Dow and co-workers (8, 33) have indicated that the formation of the α peak is not due to the isolated copper ions but to the effect of surface oxygen vacancies of an oxygen-ion-conducting support. Based on the above discussions, we further elucidate here that the α-peak formation is very likely due to the release and carrying away by CO of the surface lattice oxygen of CuO at the interface between copper oxide cluster and oxygen vacancies of SDC, such as that illustrated in steps b–c of the reaction mechanism.

The results in Table 1 reveal that the fraction of the α peak decreases with increased copper loading. The fraction of the α peak can be viewed as the number of α-type lattice oxygens needed to ignite those of other types, i.e., the $(\beta + \gamma)$-type lattice oxygen. In a low-temperature regime, the rate of reduction is controlled by the number and fraction of α-type lattice oxygen. After having been triggered by the α-type reduction reaction, the $(\beta + \gamma)$-type lattice oxygen then plays a major role in determining reduction rates, as illustrated by step f of the mechanism proposed earlier.

5. CONCLUSION

CO oxidation catalyzed by copper oxides supported on samaria-doped ceria (SDC) has been studied. On the basis of the results in this work, a preliminary mechanism involving surface lattice oxygen of CuO and oxygen vacancy participation, which leads to activity enhancement and light-off behavior, has been proposed and the following conclusions can be drawn.

1. Reducibility and susceptibility of change of oxidation states of copper oxides is key to the catalytic activities of CO oxidation. The catalytic activities depend on the propensity of copper oxide species toward valence variations and, hence, the facility of withdrawal of their surface lattice oxygen. The nonstoichiometric metastable copper oxide species formed during reduction are very active in the course of CO oxidation because of its superior ability to transport surface lattice oxygen.

2. The reduction of copper oxides has been shown to be affected to some extent by the prevailing reduction atmosphere. The reduction of copper oxide takes place more readily when CO concentration is increased in the reducing gas. However, for CuO/SDC catalysts, there is no significant difference in the kickoff temperature of α-peak reduction since the formation of α peak is attributed to the effect of surface oxygen vacancies of the oxygen-ion-conducting support. As long as it attains a certain incipient temperature, the oxygen vacancies provided by SDC are able to trigger the reduction of neighboring CuO species. An IMOSI mechanism is involved at the inception of the reduction, followed by the induced successive reduction of the bulk copper oxides.

3. The conditions for the occurrence of light-off are primarily that (i) the reaction temperature must be elevated enough and (ii) the reactant molecules participating in the reaction must be sufficient in number. Both of these conditions are associated with the turnover frequency (TOF) of the reaction, which increases considerably during light-off. The cause of light-off was attributed to the formation of coshared oxygen ions coupled with the creation of high TOF active sites which are composed of metastable copper species and two types of oxygen vacancies, i.e., $V_{o,CuO}$ and $V_{o,SDC}$. At high TOF, activities and conversions can be maintained at elevated levels.

4. Copper oxides supported on fluorite-type oxygen-ion-conducting oxides, or specifically SDC, exhibit significant light-off behavior. A negligible induction period and appreciable activity at low temperatures are characteristic of these catalysts. These are attributed to the surface oxygen vacancies of SDC facilitating the withdrawal by CO of the surface lattice oxygen of CuO at the interface between the copper oxide species and the oxygen vacancies of SDC, lowering the reduction temperature of copper oxides. Once ignited by the surface oxygen vacancy of SDC, the activity enhancement and light-off behavior can be attributed to the oxygen vacancies of CuO and $(\beta + \gamma)$-type CuO clusters. Over these CuO/SDC catalysts, the active sites composed of metastable copper species and two types of oxygen vacancies exhibit the Langmuir–Hinshelwood-type mechanism although the redox-cycle mechanism is still operative.

REFERENCES

1. Kummer, J. T., *Prog. Energy Combust. Sci.* **6**, 177 (1980).
2. Huang, T. J., and Yu, T.-C., *Appl. Catal.* **71**, 275 (1991).
3. Tauster, S. J., Fung, S. C., and Garten, R. L., *J. Am. Chem. Soc.* **100**, 170 (1978).
4. Stevenson, S. A., Dumesic, J. A., Baker, R. T. K., and Ruckenstein, E., Eds., "Metal–Support Interaction in Catalysis, Sintering, and Redispersion." Van Nostrand–Reinhold, New York, 1987.
5. Burch, R., and Flambard, A. R., *J. Catal.* **78**, 389 (1982).
6. Metcalfe, I. S., and Sundaresan, S., *AIChE J.* **34**, 195 (1988).

7. Cho, B. K., *J. Catal.* **131**, 74 (1991).
8. Dow, W. P., and Huang, T. J., *J. Catal.* **160**, 171 (1996).
9. Wang, J. B., Shih, W.-H., and Huang, T. J., *Appl. Catal. A* **203**, 191 (2000).
10. Silver, R. G., Hou, C. J., and Ekerdt, J. G., *J. Catal.* **118**, 400 (1989).
11. Dilara, P. A., and Vohs, J. M., *J. Phys. Chem.* **97**, 12919 (1993).
12. Roozeboom, F., Jos van Dillen, A., Geus, J. W., and Gellings, P. J., *Ind. Eng. Chem. Prod. Res. Dev.* **20**, 304 (1981).
13. Boon, A. Q. M., van Looij, F., and Geus, J. W., *J. Mol. Catal.* **75**, 277 (1992).
14. Yao, H. C., and Yu Yao, Y. F., *J. Catal.* **86**, 254 (1984).
15. Summers, J. C., and Ausen, S. A., *J. Catal.* **58**, 131 (1979).
16. Choudhary, C. B., Maiti, H. S., and Subbarao, E. C., *in* "Solid Electrolytes and Their Applications" (E. C. Subbarao, Ed.), p. 47. Plenum, New York, 1980.
17. Kubsh, J. E., Rieck, J. S., and Spencer, N. D., *in* "Catalysis and Automotive Pollution Control II" (A. Crucq, Ed.), p. 125. Elsevier, Amsterdam, 1991.
18. Etsell, T. H., and Flengas, S. N., *Chem. Rev.* **70**, 339 (1970).
19. Maitra, A. M., *Appl. Catal. A* **104**, 11 (1993).
20. Spivey, J. J., *Ind. Eng. Chem. Res.* **26**, 2165 (1987).
21. Satterfield, C. N., "Heterogeneous Catalysis in Industrial Practice," 2nd ed. McGraw–Hill, New York, 1991.
22. Liu, W., Sarofim, A. F., and Flytzani-Stephanopoulos, M., *Chem. Eng. Sci.* **49**, 4871 (1994).
23. Yahiro, H., Eguchi, Y., Eguchi, K., and Arai, H., *J. Appl. Electrochem.* **18**, 527 (1988).
24. Jones, A., and McNicol, B., "Temperature-Programmed Reduction for Solid Materials Characterization." Dekker, New York, 1986.
25. Severino, F., Brito, J. L., Laine, J., Fierro, J. L. G., and Lopez Agudo, A., *J. Catal.* **177**, 82 (1998).
26. Shih, W.-H., M.S. thesis. Dept. Chem. Eng., National Tsing Hua Univ., Taiwan, R.O.C., 1995 (in Chinese).
27. Jin, T., Okuhara, T., Mains, G. J., and White, J. M., *J. Phys. Chem.* **91**, 3310 (1987).
28. Serre, C., Garin, F., Belot, G., and Marie, G., *J. Catal.* **141**, 9 (1993).
29. Bielañski, A., and Haber, J., *in* "Oxygen in Catalysis," p. 244. Dekker, New York, 1991.
30. Jernigan, G. G., and Somorjai, G. A., *J. Catal.* **147**, 567 (1994).
31. Golodets, G. I., *in* "Heterogeneous Catalytic Reactions Involving Molecular Oxygen," p. 280. Elsevier, Amsterdam, 1983.
32. Boreskov, G. K., *in* "Catalysis: Science and Technology" (J. R. Anderson and M. Boudart, Eds.), Vol. 3, p. 40. Springer-Verlag, Berlin/Heidelberg, 1982.
33. Dow, W. P., Wang, Y. P., and Huang, T. J., *J. Catal.* **160**, 155 (1996).
34. Dow, W. P., and Huang, T. J., *J. Catal.* **147**, 322 (1994).
35. Lo Jacono, M., Cimino, A., and Inversi, M., *J. Catal.* **76**, 320 (1982).
36. Pierron, E. D., Rashkin, J. A., and Roth, J. F., *J. Catal.* **9**, 38 (1967).
37. Choi, K. I., and Vannice, M. A., *J. Catal.* **131**, 22 (1991).
38. Panayotov, D., and Mehandjiev, D., *Stud. Surf. Sci. Catal.* **75**, 1449 (1983).
39. Sakurai, K., Okamoto, Y., Imanaka, T., and Teranishi, S., *Bull. Chem. Soc. Jpn.* **49**, 1732 (1976).
40. Liu, W., and Flytzani-Stephanopoulos, M., *Chem. Eng. J.* **64**, 283 (1996).
41. Liu, W., and Flytzani-Stephanopoulos, M., *J. Catal.* **153**, 304 (1995).
42. Skårman, B., Reine Wallenberg, L., Larsson, P.-O., Andersson, A., Bovin, J.-O., Jacobsen, S. N., and Helmersson, U., *J. Catal.* **181**, 6 (1999).
43. Sadykov, V. A., and Tikhov, S. F., *J. Catal.* **165**, 279 (1997).
44. Nagase, K., Zheng, Y., Kodama, Y., and Kakuta, J., *J. Catal.* **187**, 123 (1999).
45. Dekker, N. J. J., Hoorn, A. J. J., Stegenga, S., Kapteijn, F., and Moulijn, J. A., *AIChE J.* **38**, 385 (1992).
46. Zhang, Z., Verykios, X. E., and Baerns, M., *Catal. Rev.–Sci. Eng.* **36**, 507 (1994).
47. Mergler, Y. J., van Aalst, A., van Delft, J., and Nieuwenhuys, B. E., *Appl. Catal. B* **10**, 245 (1996).
48. Voge, H. H., and Atkins, L. T., *J. Catal.* **1**, 171 (1962).
49. Klissurski, D., and Rives, V., *Appl. Catal. A* **109**, 1 (1994).
50. Deo, G., and Wachs, I. E., *J. Catal.* **146**, 323 (1994).
51. Liu, W., and Flytzani-Stephanopoulos, M., *J. Catal.* **153**, 317 (1995).